RESEARCH PAPER
*Future Research in AI & IoT, 2025, 1(2)*
*Homepage: https://frai.journals.umz.ac.ir/*
*DOI:*

# Multi-Dimensional Color Space Analysis with Deep Neural Network Architectures for Precision Breast Cancer Diagnosis

**Salehe Rahmanimotlagh[1], Faridoddin Rahmanimotlagh[2]*, Mohammad Mahdi Khalilzadeh[1]**

[1]*Department of Biomedical Engineering, Mashhad Branch, Islamic Azad University, Mashhad, Iran,*
[2]*Department of Mechanical Engineering, Ferdowsi University of Mashhad, Mashhad, Iran,*

**Article Info**
Received -----
Accepted -----
Available online -----

**Keywords:**
Breast Cancer Detection;
Computer-Aided Diagnosis;
Convolutional Neural Network;
Color Space;
Pattern Recognition.

**Abstract:**
Early detection of cancer can significantly increase life expectancy. Accordingly, in recent years, there has been remarkable development in the progress of computer-aided diagnosis (CAD) systems to assist physicians and specialists. The use of histopathological images in breast cancer diagnosis is considered the gold standard; therefore, CAD systems that utilize histopathological images can be highly effective in supporting physicians' diagnoses. In this study, we employed various pre-trained deep networks such as VGG, ResNet, Xception, and InceptionResNet to detect and classify microscopic images from the BACH breast cancer dataset. Our goal was to provide a comprehensive comparison of different methods based on evaluation metrics, including accuracy, F1-score, recall, and precision. The main innovation of this thesis lies in examining the effect of choosing different color spaces, such as RGB, YCbCr, and HSV, on the performance of the utilized networks. Our objective in this comparison is to select a color space that mimics the human eye (pathologist) as closely as possible. The findings of this study show that utilizing and integrating features from different layers of convolutional networks significantly improves network performance. Ultimately, for binary classification using the InceptionResNet network, feature fusion layer, and fully connected layer in the HSV color space, a classification accuracy of 92% was achieved. For four-class classification using the Inception network, feature fusion layer, and fully connected layer in the HSV color space, a classification accuracy of 86% was obtained.



***Corresponding Author:** faridodin.rahmanimotlagh@alumni.um.ac.ir

**Supplementary information:** Supplementary information for this article is available at https://frai.journals.umz.ac.ir/
**Please cite this paper as:**

## 1. Introduction

Cancer is characterized by the uncontrolled growth and abnormal spread of cells in the body [1]. It can begin in any part of the body. One type of cancer that, according to the World Health Organization (WHO), has seen a rise in prevalence among women in recent years is breast cancer [2]. According to statistics reported in 2024, 2.3 million new cases were diagnosed [3]. On average, 2.1 million women are affected by this type of cancer each year, and unfortunately, it accounts for approximately 15% (9.6 million) of cancer-related deaths [4]. However, when detected early, this disease is treatable in 98% of cases [5]. Effective methods for diagnosing this disease include imaging-based techniques such as X-ray, Computed Tomography (CT), magnetic resonance imaging (MRI), and ultrasound [6]. However, these methods can only detect the presence of a mass in the breast tissue and cannot identify its type [7]. The only method capable of determining the type of tumor is tissue biopsy and analysis of microscopic images. Biopsy and diagnosis based on histopathological images are performed by a pathologist [8]. The accuracy of diagnosis from these images largely depends on the knowledge, expertise, and experience of the pathologist [9].



*ISSN*

Computer-aided diagnosis (CAD) systems developed by researchers can assist physicians or pathologists in this task [10, 11]. In recent years, automated CAD systems leveraging deep learning, especially convolutional neural networks (CNNs), have shown promising capabilities in classifying histopathological images with high accuracy and consistency [12, 13]. The BACH histopathological dataset, comprising diverse breast tissue classes at high magnification, provides an excellent benchmark for evaluating such methods [14, 15]. In this study, we conduct a comprehensive evaluation of several pre-trained CNN architectures across multiple color spaces, combined with feature fusion techniques, to improve breast cancer classification accuracy. Our approach highlights the critical role of color representation and network architecture in diagnostic performance and offers valuable insights toward developing reliable clinical decision-support systems.

### 1.1. Breast Cancer

Breast cancer is defined by the uncontrolled proliferation and division of cancerous cells within breast tissue, usually originating from the cells lining the milk ducts, leading to the formation of a tumor [16]. This type of cancer commonly affects women, though men can also be diagnosed with it. The causes of breast cancer can be categorized into two groups: non-modifiable factors (such as genetics, being female, genetic mutations, family history, and ethnicity) and modifiable factors (such as smoking, alcohol consumption, and being overweight). The female breast consists of lobes and lobules, milk ducts, and stroma. Lobes and lobules are the glands responsible for milk production. Women's breasts typically contain more glandular tissue than men's [17]. A woman's breast includes 12–20 lobes, which are divided by fibrous tissue and positioned in a radial pattern around the nipple. A lobe is a section of the breast, bounded by grooves, fissures, connective tissue, or other anatomical structures, and is observable without the aid of a microscope [18]. Each lobe is composed of many smaller lobules, which contain milk-producing glands (alveoli) at their ends [19]. Milk is produced in these alveoli in response to hormonal signals. The lobules are connected to the nipple by thin tubes (1–2 mm in diameter) called milk ducts, which transport milk from the alveoli to the areola —the darker region surrounding the nipple at the center of the breast. From the areola, the ducts merge into larger ducts (up to 4 mm in diameter) that lead to the nipple [20]. The fibrous connective and adipose tissues, collectively referred to as the stroma, constitute the primary components of breast tissue, occupying the spaces between the lobules and ducts [21]. These connective tissues, along with suspensory ligaments, provide structural support and contribute to the breast's shape and volume. The type of breast cancer depends on which part of the breast tissue becomes cancerous. It most commonly starts in the cells lining the milk ducts. However, it can also develop in various parts of the breast, including the lobules, milk ducts, or sometimes in the spaces between tissues [22].

## 2. Methods and Materials

In this section, the proposed method presented in this research is described. The overall process includes data collection, color space selection, channel separation, preprocessing, feature extraction, feature fusion, classification (binary and four-class), and evaluation.

### 2.2. Dataset

In this study, the BACH histopathological image dataset of breast cancer at 100× magnification level has been used. Compared to the previously utilized BreaKHis and Bioimaging 2015 datasets, BACH is more recent [15]. Typically, this dataset contains 100 images for each category: normal, benign, in situ carcinoma, and invasive carcinoma. These histopathological images demonstrate morphological changes from normal tissue to advanced stages of invasive carcinoma, playing a key role in pathological diagnosis. To enhance clarity and visual understanding, sample images from this dataset, illustrating different stages of the disease, are presented in Figure 1.

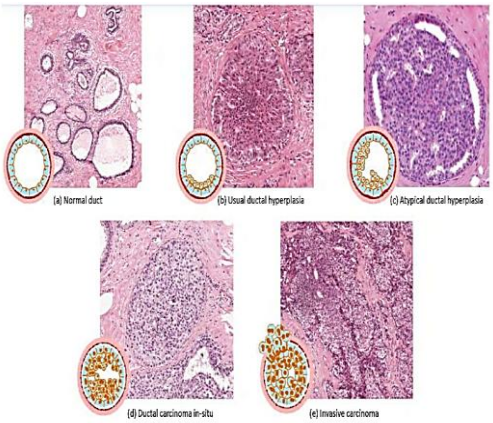


**Figure 1. Tissue changes from normal to invasive cancer: Examples of histopathology images from the BACH dataset, including (a) Normal, (b) Benign, (c) In Situ Carcinoma, and (d) Invasive Carcinoma [14, 15].**

### 2.3. Color Space Selection

For the first time in this study, different color spaces have been evaluated for breast cancer identification and categorization of breast cancer images. These color spaces include RGB, YCbCr, and HSV. One of our objectives in this study is to utilize color spaces that operate similarly to human vision, which is facilitated by the YCbCr and HSV spaces. Given that the original format of the images in the dataset is RGB, all previous studies have employed this color space for classification.

#### *2.3.1. Channel Separation*

The RGB color space consists of three channels: R (Red), G (Green), and B (Blue). The YCbCr color space includes a luminance channel (Y) and two chrominance channels (Cb for blue spectrum and Cr for red spectrum). The HSV color space includes three components: Hue (H), Saturation (S), and Value (V).

### 2.4. Preprocessing

As part of preprocessing, the input image data is normalized to a range between 0 and 1. Additionally, the images are resized from 1536×2048 to 512×512 pixels. It should be noted that no data augmentation techniques (such as rotation, flipping, scaling, or color jittering) were applied in this study [23]. The rationale behind this decision was to maintain a controlled setting in which the isolated effects of different color space transformations and feature extraction architectures could be evaluated. Additionally, this study relied on the use of pre-trained CNNs, which were trained on large-scale datasets such as ImageNet. These pre-trained models are recognized to possess generalizable feature extraction capabilities, making them more robust to limited data scenarios. However, we acknowledge that the absence of data augmentation may still impact model generalizability and robustness. Therefore, future work should incorporate augmentation strategies to further improve the resilience and performance of the classification framework.

### 2.5. Feature Extraction

Feature extraction in this study is performed with fine-tuning using transfer learning. **Table 2.1** presents the architecture used for each network, including the number of layers, non-trainable parameters (frozen layers), and the number of trainable parameters.

**Table 2.1 Specifications of the networks used.**

| | VGG16 | VGG19 | Inception V3 | Xception | InceptionResnetV2 |
|---|---|---|---|---|---|
| Total parameters | 14,714,688 | 20,024,384 | 21,802,784 | 20,861,480 | 54,336,736 |
| Trainable parameters | 7,079,424 | 9,439,232 | 6,073,536 | 10,016,336 | 54,276,192 |
| Non-trainable parameters | 7,635,264 | 10,585,152 | 15,729,248 | 10,845,144 | 60,544 |
| Total number of layers | 19 | 22 | 311 | 132 | 780 |

### 2.6. Feature Fusion

In this study, feature fusion is performed similarly to several previous works by adding a global pooling layer to the pre-trained (transfer) networks. **Table 2.2** presents the convolutional layers used for fusion, along with the dimensionality of the feature vector after adding the global pooling layers.

**Table 2.2 Specifications of the networks used**

| | VGG16 | VGG19 | InceptionV3 | Xception | InceptionResnetV2 |
|---|---|---|---|---|---|
| Layers used | ،12,417 | 12,43 ، | 51,28,18,11 ،120 ،101،74 ،184 ،152 ،249 ،216 294 ،263 | 126,36,26 | 618 ,275,18,11 |
| Feature vector | 1152 | 1152 | 2320 | 2520 | 1536 |

As detailed in **Table 2.2**, we explicitly specify the exact convolutional layer indices from each pre-trained CNN backbone that are included in the feature fusion. For instance, for InceptionResNetV2, layers numbered 275, 18, 11, and 618 are utilized, while for Xception, layers 126, 36, and 26 are selected. The full list of layers for all backbone networks, along with the dimensionality of the resulting feature vector after applying global pooling, is provided to ensure precise reproducibility of the feature fusion process for each backbone network.

### 2.7. Classifier Architecture

For classification, two approaches, binary and four-class, have been utilized. The dataset has been split in an 80/20 ratio, such that 80 images from each category are randomly selected as training images and 20 images as test images. In this research, the effectiveness of the fully connected layers positioned at the terminal stage of neural networks is compared with the performance of an SVM classifier with an RBF kernel, which is known for its high efficiency among machine learning classification methods. In this study, SVM classifiers with RBF kernels were employed for classification tasks. To select the optimal hyperparameters, including the regularization parameter CC and the kernel scale (gamma $\gamma\gamma$), a systematic grid search method was utilized. This method explored a predefined range of values for these hyperparameters to distinguish the combination that yielded the optimal accuracy on the training data. The grid search was combined with cross-validation on the training split, which enabled an effective and robust tuning process while avoiding overfitting. This approach ensured that the SVM classifier achieved optimal or near-optimal performance in comparison with the fully connected layers of the deep neural networks used in this study. It is worth noting that although hyperparameter optimization was performed systematically, future work could explore more advanced or automated search algorithms (e.g., randomized search or Bayesian optimization) and assess their impact on further improving classification accuracy and model robustness. In this study, we adopted a combined approach for model evaluation. While the dataset was initially split with an 80/20 ratio to establish an independent and unseen test set, 5-fold cross-validation was subsequently applied to the 80% training portion of the data. This approach allowed us to obtain a more robust and reliable performance estimation, particularly given the dataset size. The 5-fold cross-validation on the training data helped assess the model's stability and generalizability against variations in the training subsets, ensuring a statistically stronger performance evaluation while maintaining direct.

### 2.8. Evaluation Criteria

Evaluation metrics are defined based on the confusion matrix. Commonly used metrics for classification

evaluation include accuracy, recall, F1-score, and precision. These metrics are calculated using the parameters: True Positive (TP), True Negative (TN), False Positive (FP), and False Negative (FN). In this study, precision, recall, and F1-score values are calculated and presented per class individually using the one-versus-rest (OvR) approach, where each class is treated as the positive class against all other classes combined [24]. The metrics presented in our tables represent class-specific performance rather than aggregated scores. For each neural network and color space combination, we computed the precision, recall, and F1-score for every individual class (Class 1, Class 2, Class 3, and Class 4 in the four-class scenario, or Class 1 and Class 2 in the binary scenario) separately. However, we acknowledge that our current presentation lacks clarity regarding the overall aggregated performance across all classes. The precision, recall, and F1-score values shown are computed per class, but we did not explicitly specify whether macro-averaged, micro-averaged, or weighted-averaged metrics were used for summary reporting. For the current study, the reported values represent individual class performance, which allows for detailed analysis of model behavior across different cancer types. This approach is particularly valuable in medical diagnosis applications where understanding per-class performance is crucial for clinical decision-making.

## 3. Results

This chapter presents the simulation outcomes and the analysis of the results. For classification evaluation, the dataset is split using an 80/20 ratio. Specifically, 80 images from each category are randomly selected as training samples and 20 images as test samples. Random sampling is performed only once, and the resulting split is used consistently across all classification methods to ensure comparability. The evaluation includes the overall accuracy, precision, recall, and F1-score on a per-class basis. The experiment is conducted once for the binary classification case (cancerous/non-cancerous) and once for the four-class classification.

### 3.1. Classification Results

This section reports the evaluation results for the binary classification setting. In binary classification, the first class corresponds to non-cancerous samples, and the second class corresponds to cancerous samples. As mentioned, three different color spaces, RGB, YCbCr, and HSV are employed in the current study.

#### *3.2.1. Binary Classifier Results in the RGB Color Space*

**Tables 3.1** and **Tables 3.2** show the results of binary classification in the RGB color space using pre-trained neural networks with a fully connected final layer and SVM with an RBF kernel, respectively.

**Table 3.1: Results from two-class classification in RGB space and fully connected layer.**

| | F1-score | Recall | Precision | Neural Network | Accuracy |
|---|---|---|---|---|---|
| Class 1 | 0.84 | 0.81 | 0.87 | VGG16 | 0.87 |
| Class 2 | 0.85 | 0.88 | 0.82 | | |
| Class 1 | 0.67 | 0.53 | 0.89 | VGG19 | 0.86 |
| Class 2 | 0.78 | 0.94 | 0.67 | | |
| Class 1 | 0.87 | 0.84 | 0.86 | Xception | 0.86 |
| Class 2 | 0.85 | 0.88 | 0.86 | | |
| Class 1 | 0.85 | 0.78 | 0.93 | Inception | 0.87 |
| Class 2 | 0.87 | 0.94 | 0.81 | | |
| Class 1 | 0.88 | 0.88 | 0.88 | InceptionResnet | 0.88 |
| Class 2 | 0.88 | 0.88 | 0.88 | | |

Based on **Table 3.1**, utilizing the feature vector extracted from the InceptionResNet network has resulted in higher accuracy. The models VGG16, VGG19, Xception, and Inception exhibit similar accuracy, with a marginal difference of 1 to 2% compared to InceptionResNet (0.88). Given this minimal difference, it is essential to evaluate additional performance metrics. Observations indicate that certain models tend to classify data predominantly into a specific class. Here, Class 1 represents non-cancerous samples, and models VGG16, VGG19, and Inception have classified a higher number of cancerous samples as non-cancerous, which is undesirable. This misclassification may lead to delayed cancer diagnosis, thereby posing a significant threat to patients' lives. In contrast, the InceptionResNet network, with an accuracy of 0.88 for both classes, has demonstrated the best performance based on evaluation metrics. Additionally, according to the results in the table, the Xception network ranks second in terms of performance.

**Table 3.2: Results of Binary Classification in the RGB Space Using SVM with an RBF Kernel.**

| | F1-score | Recall | Precision | Neural Network | Accuracy |
|---|---|---|---|---|---|
| Class 1 | 0.75 | 0.70 | 0.80 | VGG16 | 0.76 |
| Class 2 | 0.78 | 0.82 | 0.73 | | |
| Class 1 | 0.71 | 0.68 | 0.75 | VGG19 | 0.72 |
| Class 2 | 0.74 | 0.78 | 0.70 | | |
| Class 1 | 0.81 | 0.75 | 0.88 | Xception | 0.82 |
| Class 2 | 0.84 | 0.90 | 0.78 | | |
| Class 1 | 0.73 | 0.65 | 0.84 | Inception | 0.76 |
| Class 2 | 0.79 | 0.88 | 0.71 | | |
| Class 1 | 0.65 | 0.53 | 0.84 | InceptionResnet | 0.71 |
| Class 2 | 0.76 | 0.90 | 0.65 | | |

As shown in **Table 3.2**, when using the SVM classifier, the highest accuracy (0.82) was achieved with the feature vector extracted from the Xception network. However, this accuracy is lower compared to the results in **Table 3.1**, indicating that none of the utilized networks performed satisfactorily when combined with SVM.

### *3.2.2. Analysis of Binary Classification Results in the YCbCr Color Space*

**Table 3.3** and **Table 3.4** summarize the results of binary classification in the YCbCr color space, respectively, using pre-trained neural networks with a fully connected final layer and SVM with an RBF kernel.

**Table 3.3: Results of Binary Classification in the YCbCr Color Space Using a Fully Connected Layer.**

| | F1-score | Recall | Precision | Neural Network | Accuracy |
|---|---|---|---|---|---|
| Class 1 | 0.79 | 0.75 | 0.83 | VGG16 | 0.81 |
| Class 2 | 0.81 | 0.84 | 0.77 | | |
| Class 1 | 0.83 | 0.81 | 0.84 | VGG19 | 0.83 |
| Class 2 | 0.83 | 0.84 | 0.82 | | |
| Class 1 | 0.85 | 0.78 | 0.93 | Xception | 0.87 |
| Class 2 | 0.87 | 0.94 | 0.81 | | |
| Class 1 | 0.83 | 0.75 | 0.92 | Inception | 0.84 |
| Class 2 | 0.86 | 0.94 | 0.79 | | |
| Class 1 | 0.88 | 0.88 | 0.88 | InceptionResnet | 0.88 |
| Class 2 | 0.88 | 0.88 | 0.88 | | |

As shown in **Table 3.3**, the highest accuracy (0.88) was achieved using the feature vector extracted from the InceptionResNet network. Since all the obtained values for this network are identical to those in **Table 3.1**, it can be concluded that neither the RGB nor YCbCr color spaces demonstrated superiority in this classification approach.

**Table 3.4: Results of Binary Classification in the YCbCr Color Space Using SVM with an RBF Kernel.**

| | F1-score | Recall | Precision | Neural Network | Accuracy |
|---|---|---|---|---|---|
| Class 1 | 0.65 | 0.53 | 0.84 | VGG16 | 0.71 |
| Class 2 | 0.76 | 0.90 | 0.65 | | |
| Class 1 | 0.80 | 0.40 | 0.53 | VGG19 | 0.65 |
| Class 2 | 0.60 | 0.90 | 0.72 | | |
| Class 1 | 0.77 | 0.85 | 0.77 | Xception | 0.80 |
| Class 2 | 0.83 | 0.75 | 0.83 | | |
| Class 1 | 0.92 | 0.28 | 0.42 | Inception | 0.62 |

| | | | | | |
|---|---|---|---|---|---|
| Class 2 | 0.57 | 0.97 | 0.72 | | |
| Class 1 | 0.82 | 0.82 | 0.82 | InceptionResnet | 0.82 |
| Class 2 | 0.82 | 0.82 | 0.82 | | |

As shown in **Table 3.4**, when using the SVM classifier, the highest accuracy (0.82) was achieved with the feature vector extracted from the InceptionResNet network. However, this accuracy is lower compared to **Table 3.3**, indicating that none of the utilized networks performed satisfactorily in combination with SVM within the YCbCr color space.

### *3.2.3. Analysis of Binary Classification Outcomes in the HSV Color Space*

**Table 3.5** and **Table 3.6** respectively, present the results of binary classification in the HSV color space using pre-trained neural networks with a fully connected final layer and SVM with an RBF kernel.

**Table 3.5: Results of Binary Classification in the HSV Color Space Using a Fully Connected Layer.**

| | F1-score | Recall | Precision | Neural Network | Accuracy |
|---|---|---|---|---|---|
| Class 1 | 0.69 | 0.62 | 0.77 | VGG16 | 0.75 |
| Class 2 | 0.74 | 0.81 | 0.68 | | |
| Class 1 | 0.59 | 0.50 | 0.73 | VGG19 | 0.75 |
| Class 2 | 0.70 | 0.81 | 0.62 | | |
| Class 1 | 0.86 | 0.78 | 0.96 | Xception | 0.88 |
| Class 2 | 0.89 | 0.97 | 0.82 | | |
| Class 1 | 0.86 | 0.78 | 0.96 | Inception | 0.88 |
| Class 2 | 0.89 | 0.97 | 0.82 | | |
| Class 1 | 0.90 | 0.88 | 0.93 | InceptionResnet | 0.91 |
| Class 2 | 0.91 | 0.94 | 0.88 | | |

As shown in **Table 3.5**, the highest accuracy (0.91) was achieved using the feature vector extracted from the InceptionResNet network. The accuracy obtained with this network and a fully connected layer in the RGB and YCbCr color spaces was 0.88. Given that the Inception and Xception networks also yielded higher accuracy in this space for binary classification, it can be concluded that the HSV color space is more suitable for visualization, analysis, and feature extraction from histopathology images. Within this color space, the VGG16 and VGG19 networks demonstrated lower accuracy compared to other color spaces. This suggests that both color space selection and network architecture play a crucial role. To achieve an optimized system, it is essential to consider both factors when selecting the best combination.

**Table 3.6: Results of Binary Classification in the HSV Color Space Using SVM with an RBF Kernel.**

| | F1-score | Recall | Precision | Neural Network | Accuracy |
|---|---|---|---|---|---|
| Class 1 | 0.74 | 0.70 | 0.78 | VGG16 | 0.75 |
| Class 2 | 0.76 | 0.80 | 0.73 | | |
| Class 1 | 0.74 | 0.70 | 0.78 | VGG19 | 0.75 |
| Class 2 | 0.76 | 0.80 | 0.73 | | |
| Class 1 | 0.81 | 0.78 | 0.84 | Xception | 0.81 |
| Class 2 | 0.82 | 0.85 | 0.79 | | |
| Class 1 | 0.66 | 0.55 | 0.81 | Inception | 0.71 |
| Class 2 | 0.75 | 0.88 | 0.66 | | |
| Class 1 | 0.84 | 0.81 | 0.87 | InceptionResnet | 0.87 |
| Class 2 | 0.85 | 0.88 | 0.82 | | |

As shown in **Table 6-3**, when using the SVM classifier, the highest accuracy (0.87) was achieved with the feature vector obtained from the InceptionResNet network. However, this accuracy is lower than that reported in **Table 3.4**, indicating that none of the utilized networks performed better when combined with SVM compared to the fully connected layer within the HSV color space. Nevertheless, it is noteworthy

that the accuracy and other evaluation metrics obtained in this method for the HSV space were superior to those of other color spaces, highlighting the effectiveness of this color representation.

### *3.2.4 Analysis of Feature Fusion in Binary Classification*

Since classification using a fully connected layer provided better results compared to SVM, classification in this method was performed using feature fusion of convolutional layers before the pooling layer. The results of this approach are presented in the following section.

**Table 3.7: Results of Binary Classification in the RGB Color Space Using a Fully Connected Layer with Feature Fusion.**

| | F1-score | Recall | Precision | Neural Network | Accuracy |
|---|---|---|---|---|---|
| Class 1 | 0.80 | 0.75 | 0.86 | VGG16 | 0.89 |
| Class 2 | 0.82 | 0.88 | 0.78 | | |
| Class 1 | 0.81 | 0.72 | 0.92 | VGG19 | 0.83 |
| Class 2 | 0.85 | 0.94 | 0.77 | | |
| Class 1 | 0.89 | 0.84 | 0.93 | Xception | 0.87 |
| Class 2 | 0.90 | 0.94 | 0.86 | | |
| Class 1 | 0.89 | 0.88 | 0.90 | Inception | 0.89 |
| Class 2 | 0.89 | 0.91 | 0.88 | | |
| Class 1 | 0.96 | 0.81 | 0.96 | InceptionResnet | 0.90 |
| Class 2 | 0.84 | 0.97 | 0.96 | | |

As shown in this table, using the feature vector extracted from the InceptionResNet network resulted in higher accuracy (0.90) and precision (0.96) for both classes. This accuracy surpasses the previously obtained value (0.88) in this space, indicating the effectiveness of feature fusion. It is observed that in all utilized networks (except VGG19), feature fusion has led to an improvement in accuracy and other evaluation metrics.

**Table 3.8: Results of Binary Classification in the YCbCr Color Space Using a Fully Connected Layer with Feature Fusion.**

| | F1-Score | Recall | Precision | Neural Network | Accuracy |
|---|---|---|---|---|---|
| Class 1 | 0.78 | 0.80 | 0.76 | VGG16 | 0.83 |
| Class 2 | 0.86 | 0.84 | 0.87 | | |
| Class 1 | 0.76 | 0.85 | 0.68 | VGG19 | 0.79 |
| Class 2 | 0.81 | 0.75 | 0.89 | | |
| Class 1 | 0.85 | 0.78 | 0.93 | Xception | 0.88 |
| Class 2 | 0.87 | 0.94 | 0.81 | | |
| Class 1 | 0.86 | 0.84 | 0.87 | Inception | 0.86 |
| Class 2 | 0.86 | 0.88 | 0.85 | | |
| Class 1 | 0.87 | 0.83 | 0.96 | InceptionResnet | 0.90 |
| Class 2 | 0.86 | 0.88 | 0.90 | | |

As shown in this table, feature fusion of convolutional layers in the YCbCr color space has also led to an improvement in classification accuracy and precision. The highest accuracy (0.90) was achieved using the feature vector obtained from the InceptionResNet network. Similar to the results observed in the non-fusion approach, there is no significant difference in accuracy between the RGB and YCbCr color spaces.

**Table 3.9: Results of Binary Classification in the HSV Color Space Using a Fully Connected Layer with Feature Fusion.**

| | F1-score | Recall | Precision | Neural Network | Accuracy |
|---|---|---|---|---|---|
| Class 1 | 0.84 | 0.84 | 0.84 | VGG19 | 0.84 |
| Class 2 | 0.84 | 0.84 | 0.84 | | |
| Class 1 | 0.84 | 0.84 | 0.84 | VGG19 | 0.84 |

| | | | | | |
|---|---|---|---|---|---|
| Class 2 | 0.84 | 0.84 | 0.84 | | |
| Class 1 | 0.90 | 0.81 | 0.90 | Xception | 0.88 |
| Class 2 | 0.83 | 0.91 | 0.83 | | |
| Class 1 | 0.90 | 0.88 | 0.93 | Inception | 0.91 |
| Class 2 | 0.91 | 0.94 | 0.88 | | |
| Class 1 | 0.92 | 0.92 | 0.92 | InceptionResnet | 0.92 |
| Class 2 | 0.92 | 0.92 | 0.92 | | |

As shown in this table, in the feature fusion approach within the HSV color space, using the feature vector extracted from the InceptionResNet network resulted in the highest accuracy (0.92). This value is higher than the non-fusion scenario and also exceeds the accuracy obtained through feature fusion in the RGB and YCbCr color spaces. Overall, it can be concluded that for binary classification, the InceptionResNet network combined with a feature fusion layer and a fully connected layer demonstrated the best performance in the HSV color space.

### *3.3. Analysis of Multi-Class Classification Results*

The following part presents the evaluation results for multi-class classification scenarios. In the four-class classification, the first class represents Normal data, the second corresponds to Benign samples, the third pertains to InSitu data, and the fourth includes Invasive cases. As mentioned in the previous section, this study employs three different color spaces: RGB, YCbCr, and HSV.

#### *3.3.1. Evaluation of Four-Class Classification in the RGB Color Space*

**Table 3.10** and **Table 3.11** respectively, present the results of four-class classification in the RGB color space using pre-trained neural networks with a fully connected final layer and SVM with an RBF kernel.

**Table 3.10: Results of Four-Class Classification in the RGB Color Space Using a Fully Connected Layer.**

| | F1-score | Recall | Precision | Neural Network | Accuracy |
|---|---|---|---|---|---|
| Class 1 | 0.76 | 0.70 | 0.82 | VGG16 | 0.75 |
| Class 2 | 0.63 | 0.60 | 0.67 | | |
| Class 3 | 0.74 | 0.85 | 0.65 | | |
| Class 4 | 0.87 | 0.85 | 0.89 | | |
| Class 1 | 0.76 | 0.65 | 0.93 | VGG19 | 0.76 |
| Class 2 | 0.70 | 0.65 | 0.76 | | |
| Class 3 | 0.76 | 0.80 | 0.73 | | |
| Class 4 | 0.81 | 0.95 | 0.70 | | |
| Class 1 | 0.74 | 0.80 | 0.70 | Xception | 0.76 |
| Class 2 | 0.71 | 0.60 | 0.86 | | |
| Class 3 | 0.68 | 0.70 | 0.67 | | |
| Class 4 | 0.90 | 0.95 | 0.86 | | |
| Class 1 | 0.76 | 0.70 | 0.82 | Inception | 0.79 |
| Class 2 | 0.70 | 0.70 | 0.70 | | |
| Class 3 | 0.78 | 0.80 | 0.76 | | |
| Class 4 | 0.90 | 0.95 | 0.86 | | |
| Class 1 | 0.72 | 0.70 | 0.74 | InceptionResnet | 0.77 |
| Class 2 | 0.62 | 0.60 | 0.63 | | |
| Class 3 | 0.80 | 0.80 | 0.80 | | |
| Class 4 | 0.95 | 1 | 0.91 | | |

As shown in this table, using the feature vector extracted from the Inception network resulted in higher accuracy

(0.79). The obtained accuracy values differ by 0.04 across the utilized networks.

**Table 3.11: Results of Four-Class Classification in the RGB Color Space Using SVM with an RBF Kernel.**

| | F1-score | Recall | Precision | Neural Network | Accuracy |
|---|---|---|---|---|---|
| Class 1 | 0.70 | 0.75 | 0.65 | VGG16 | 0.58 |
| Class 2 | 0.50 | 0.45 | 0.56 | | |
| Class 3 | 0.57 | 0.50 | 0.67 | | |
| Class 4 | 0.57 | 0.65 | 0.50 | | |
| Class 1 | 0.70 | 0.65 | 0.76 | VGG19 | 0.70 |
| Class 2 | 0.70 | 0.65 | 0.76 | | |
| Class 3 | 0.57 | 0.50 | 0.67 | | |
| Class 4 | 0.78 | 1 | 0.65 | | |
| Class 1 | 0.68 | 0.70 | 0.67 | Xception | 0.66 |
| Class 2 | 0.48 | 0.40 | 0.62 | | |
| Class 3 | 0.68 | 0.65 | 0.72 | Inception | 0.53 |
| Class 4 | 0.75 | 0.90 | 0.64 | | |
| Class 1 | 0.62 | 0.50 | 0.83 | | |
| Class 2 | 0.42 | 0.40 | 0.44 | | |
| Class 3 | 0.44 | 0.40 | 0.50 | | |
| Class 4 | 0.63 | 0.85 | 0.50 | | |
| Class 1 | 0.65 | 0.70 | 0.61 | InceptionResnet | 0.73 |
| Class 2 | 0.70 | 0.75 | 0.65 | | |
| Class 3 | 0.74 | 0.70 | 0.78 | | |
| Class 4 | 0.83 | 0.75 | 0.94 | | |

As shown in this table, using the feature vector extracted from the InceptionResNet network resulted in an accuracy of 0.73. While this is the highest accuracy recorded in this table, it is lower than the accuracy obtained through classification using a fully connected layer. Overall, it can be concluded that in four-class classification, SVM with an RBF kernel has not demonstrated satisfactory performance.

### *3.3.2. Evaluation of Four-Class Classification in the YCbCr Color Space*

**Table 3.12** to **Table 3.13** present the results of four-class classification in the YCbCr color space using pre-trained neural networks with a fully connected final layer and SVM with an RBF kernel, respectively.

**Table 3.12: Results of Four-Class Classification in the YCbCr Color Space Using a Fully Connected Layer.**

| | F1-score | Recall | Precision | Neural Network | Accuracy |
|---|---|---|---|---|---|
| Class 1 | 0.58 | 0.70 | 0.50 | VGG16 | 0.60 |
| Class 2 | 0.53 | 0.45 | 0.64 | | |
| Class 3 | 0.68 | 0.75 | 0.62 | | |
| Class 4 | 0.59 | 0.50 | 0.71 | | |
| Class 1 | 0.46 | 0.80 | 0.46 | VGG19 | 0.60 |
| Class 2 | 0.86 | 0.30 | 0.86 | | |
| Class 3 | 0.55 | 0.55 | 0.55 | | |
| Class 4 | 0.83 | 0.75 | 0.75 | | |
| Class 1 | 0.80 | 0.90 | 0.72 | Xception | 0.76 |
| Class 2 | 0.61 | 0.50 | 0.77 | | |

| | | | | | |
|---|---|---|---|---|---|
| Class 3 | 0.75 | 0.75 | 0.75 | | |
| Class 4 | 0.86 | 0.90 | 0.82 | | |
| Class 1 | 0.72 | 0.90 | 0.72 | | |
| Class 2 | 0.77 | 0.50 | 0.77 | | |
| Class 3 | 0.75 | 0.75 | 0.75 | Inception | 0.76 |
| Class 4 | 0.82 | 0.90 | 0.82 | | |
| Class 1 | 0.83 | 0.85 | 0.81 | | |
| Class 2 | 0.57 | 0.50 | 0.67 | | |
| Class 3 | 0.67 | 0.75 | 0.60 | InceptionResnet | 0.71 |
| Class 4 | 0.77 | 0.75 | 0.79 | | |

As shown in this table, the highest accuracy obtained is 0.76, achieved using the feature vector extracted from the Inception and Xception networks. However, this value is lower than the result obtained in the RGB color space (0.79).

**Table 3.13: Results of Four-Class Classification in the YCbCr Color Space Using SVM with an RBF Kernel.**

| | F1-score | Recall | Precision | Neural Network | Accuracy |
|---|---|---|---|---|---|
| Class 1 | 0.44 | 0.35 | 0.58 | | |
| Class 2 | 0.48 | 0.55 | 0.42 | | |
| Class 3 | 0.50 | 0.45 | 0.56 | VGG16 | 0.52 |
| Class 4 | 0.65 | 0.75 | 0.58 | | |
| Class 1 | 0.63 | 0.75 | 0.54 | | |
| Class 2 | 0.48 | 0.35 | 0.78 | VGG19 | 0.64 |
| Class 3 | 0.65 | 0.65 | 0.65 | | |
| Class 4 | 0.74 | 0.80 | 0.70 | | |
| Class 1 | 0.55 | 0.80 | 0.55 | | |
| Class 2 | 0.60 | 0.30 | 0.60 | | |
| Class 3 | 0.63 | 0.60 | 0.63 | Xception | 0.62 |
| Class 4 | 0.73 | 0.80 | 0.73 | | |
| Class 1 | 0.60 | 0.70 | 0.52 | | |
| Class 2 | 0.48 | 0.40 | 0.62 | | |
| Class 3 | 0.53 | 0.45 | 0.64 | Inception | 0.56 |
| Class 4 | 0.61 | 0.70 | 0.54 | | |
| Class 1 | 0.79 | 0.75 | 0.79 | | |
| Class 2 | 0.86 | 0.30 | 0.86 | | |
| Class 3 | 0.57 | 0.85 | 0.57 | InceptionResnet | 0.66 |
| Class 4 | 0.62 | 0.75 | 0.62 | | |

As shown in this table, using the feature vector extracted from the InceptionResNet network resulted in an accuracy of 0.66. While this is the highest accuracy recorded in this table, it is lower than the results obtained through classification using a fully connected layer. Overall, it can be concluded that in four-class classification within the YCbCr color space, SVM with an RBF kernel has not demonstrated satisfactory performance.

### *3.3.3. Evaluation of Four-Class Classification in the HSV Color Space*

**Table 3.14** presents the results of four-class classification in the HSV color space using pre-trained neural networks with a fully connected final layer and SVM with an RBF kernel.

**Table 3.14: Results of Four-Class Classification in the HSV Color Space Using a Fully Connected Layer.**

| | F1-score | Recall | Precision | Neural Network | Accuracy |
|---|---|---|---|---|---|
| Class 1 | 0.68 | 0.70 | 0.67 | VGG16 | 0.65 |
| Class 2 | 0.59 | 0.50 | 0.71 | | |
| Class 3 | 0.61 | 0.70 | 0.54 | | |
| Class 4 | 0.72 | 0.70 | 0.74 | | |
| Class 1 | 0.50 | 0.55 | 0.46 | VGG19 | 0.51 |
| Class 2 | 0.55 | 0.45 | 0.69 | | |
| Class 3 | 0.40 | 0.45 | 0.36 | | |
| Class 4 | 0.63 | 0.60 | 0.67 | | |
| Class 1 | 0.67 | 0.85 | 0.55 | Xception | 0.71 |
| Class 2 | 0.60 | 0.45 | 0.90 | | |
| Class 3 | 0.76 | 0.80 | 0.73 | | |
| Class 4 | 0.81 | 0.75 | 0.88 | | |
| Class 1 | 0.87 | 0.85 | 0.89 | Inception | 0.80 |
| Class 2 | 0.65 | 0.55 | 0.79 | | |
| Class 3 | 0.81 | 0.85 | 0.77 | | |
| Class 4 | 0.84 | 0.95 | 0.76 | | |
| Class 1 | 0.84 | 0.95 | 0.76 | InceptionResnet | 0.78 |
| Class 2 | 0.57 | 0.40 | 1 | | |
| Class 3 | 0.74 | 0.80 | 0.70 | | |
| Class 4 | 0.86 | 0.95 | 0.79 | | |

As shown in this table, using the feature vector extracted from the Inception network resulted in an accuracy of 0.80. The obtained accuracy in the HSV color space is higher compared to RGB (0.79) and YCbCr (0.76). Notably, while InceptionResNet achieved the best results in binary classification, in four-class classification using a fully connected layer, the Inception network yielded the highest accuracy.

**Table 3.15: Results of Four-Class Classification in the HSV Color Space Using SVM with an RBF Kernel.**

| | F1-score | Recall | Precision | Neural Network | Accuracy |
|---|---|---|---|---|---|
| Class 1 | 0.58 | 0.65 | 0.52 | VGG16 | 0.61 |
| Class 2 | 0.55 | 0.45 | 0.69 | | |
| Class 3 | 0.56 | 0.55 | 0.58 | | |
| Class 4 | 0.74 | 0.80 | 0.70 | | |
| Class 1 | 0.73 | 0.75 | 0.71 | VGG19 | 0.68 |
| Class 2 | 0.65 | 0.55 | 0.79 | | |
| Class 3 | 0.59 | 0.60 | 0.57 | | |
| Class 4 | 0.73 | 0.80 | 0.67 | | |
| Class 1 | 0.72 | 0.70 | 0.74 | Xception | 0.78 |
| Class 2 | 0.70 | 0.65 | 0.76 | | |
| Class 3 | 0.78 | 0.80 | 0.76 | | |
| Class 4 | 0.88 | 0.95 | 0.83 | | |
| Class 1 | 0.55 | 0.55 | 0.55 | Inception | 0.57 |
| Class 2 | 0.56 | 0.50 | 0.62 | | |
| Class 3 | 0.48 | 0.40 | 0.62 | | |
| Class 4 | 0.67 | 0.85 | 0.55 | | |
| Class 1 | 0.78 | 0.90 | 0.69 | InceptionResnet | 0.73 |
| Class 2 | 0.53 | 0.40 | 0.80 | | |
| Class 3 | 0.77 | 0.75 | 0.79 | | |
| Class 4 | 0.76 | 0.85 | 0.68 | | |

As previously mentioned, color space selection, network architecture, and classifier choice are all critical factors in

performance evaluation and must be compared comprehensively.

### *3.3.4. Analysis of Feature Fusion in Four-Class Classification*

Similar to binary classification, in four-class classification, the results obtained using a fully connected layer were superior to those obtained using SVM. As discussed, classification was performed using feature fusion of convolutional layers before the pooling layer, and the results of this approach are presented in the following section.

**Table 3.16: Results of Four-Class Classification in the RGB Color Space Using a Fully Connected Layer with Feature Fusion.**

| | F1-score | Recall | Precision | Neural Network | Accuracy |
|---|---|---|---|---|---|
| Class 1 | 0.82 | 0.90 | 0.75 | VGG16 | 0.74 |
| Class 2 | 0.69 | 0.60 | 0.80 | | |
| Class 3 | 0.62 | 0.50 | 0.83 | | |
| Class 4 | 0.78 | 0.95 | 0.66 | | |
| Class 1 | 0.62 | 0.70 | 0.56 | VGG19 | 0.55 |
| Class 2 | 0.38 | 0.25 | 0.83 | | |
| Class 3 | 0.42 | 0.45 | 0.39 | | |
| Class 4 | 0.70 | 0.80 | 0.62 | | |
| Class 1 | 0.76 | 0.80 | 0.73 | Xception | 0.81 |
| Class 2 | 0.74 | 0.65 | 0.87 | | |
| Class 3 | 0.81 | 0.85 | 0.77 | | |
| Class 4 | 0.93 | 0.95 | 0.90 | | |
| Class 1 | 0.76 | 0.95 | 0.76 | Inception | 0.78 |
| Class 2 | 1 | 0.40 | 1 | | |
| Class 3 | 0.70 | 0.80 | 0.70 | | |
| Class 4 | 0.79 | 0.95 | 0.79 | | |
| Class 1 | 0.71 | 0.85 | 0.71 | InceptionResnet | 0.71 |
| Class 2 | 0.82 | 0.45 | 0.82 | | |
| Class 3 | 0.76 | 0.65 | 0.76 | | |
| Class 4 | 0.64 | 0.90 | 0.64 | | |

As shown in this table, in the feature fusion approach within the HSV color space, using the feature vector extracted from the Inception network resulted in the highest accuracy (0.86). This value surpasses the non-fusion scenario and also exceeds the accuracy obtained through feature fusion in the RGB and YCbCr color spaces. Overall, it can be concluded that for four-class classification, the Inception network combined with a feature fusion layer and a fully connected layer demonstrated the best performance in the HSV color space.

## 4. Discussion and Conclusion

In the current study, no interpretability methods such as Grad-CAM, SHAP, or attention maps were applied to explain the model's decisions. Incorporating such visual explainability techniques is indeed valuable for increasing clinical trust and understanding of the model's predictions. As future work, we plan to implement and analyze Grad-CAM or similar visualization methods to highlight important regions of histopathological images that contribute to classification decisions. This will provide clinicians with intuitive and informative insights to support model outputs and improve transparency in automated breast cancer diagnosis.

### *4.1. Recommendations for Future Work*

To improve this research, the following suggestions are proposed:

- Enhancing collaboration between medical experts and diagnostic systems, ensuring evaluation under expert supervision.
- Expanding the dataset to evaluate proposed methods on larger databases.
- Developing diagnostic systems capable of distinguishing more cancer subtypes.

- Combining extracted features from deep networks with physician-selected features for improved performance.
- Exploring newer deep networks to boost classification accuracy.
- Extracting features using diverse pre-trained networks and fusing layers from multiple networks.
- Incorporating segmentation techniques to analyze histopathological images before feature extraction.

With the rapid rise in breast cancer cases in recent years, the need for efficient screening and early diagnosis has become crucial. Various methods are used for breast cancer screening and diagnosis, but histopathological image analysis from biopsies remains the gold standard for identifying cancer type and stage. Traditionally, these images are analyzed by expert pathologists, but challenges such as limited access to experienced professionals and the possibility of human error necessitate the development of computer-aided diagnostic systems to improve accuracy and speed. This study utilized transfer learning-based methods for breast cancer diagnosis using histopathological images. We evaluated different pre-trained neural networks and color spaces, and our findings indicate that leveraging multiple convolutional layer features and fusing them significantly enhances model performance. Selecting the HSV color space, which describes colors similarly to human vision, led to better classification performance compared to RGB and YCbCr color spaces. In summary:

1. For binary classification, using InceptionResNet, feature fusion, and a fully connected layer within HSV resulted in 92% classification accuracy.
2. For four-class classification, using Inception, feature fusion, and a fully connected layer within HSV resulted in 86% classification accuracy.

Recent advances in automated breast cancer diagnosis using the BACH histopathology dataset have demonstrated a variety of deep learning architectures, particularly ensembles, transformer-based models, and advanced feature fusion approaches, that achieve benchmark results approaching or exceeding 97% accuracy in four-class classification. These state-of-the-art (SOTA) methods typically employ extensive data augmentation, modern lightweight networks, or hybrid CNN-Transformer models, and often leverage ensemble strategies to maximize predictive performance and robustness. The current study evaluates several pre-trained CNN backbones (VGG16, VGG19, Xception, Inception, and InceptionResNet) across different color spaces. The best performance achieved for four-class classification in this work is an accuracy of 0.86 using the Inception network with feature fusion in the HSV color space. In binary classification (cancer/non-cancer), the highest reported accuracy is 0.92 using InceptionResNet with feature fusion. The proposed approach provides competitive accuracy compared to foundational CNN approaches but falls short of the latest SOTA methods that integrate ensembles, transformers, or comprehensive augmentation. Unlike some recent studies, this work did not incorporate advanced augmentation techniques or model ensembles, which are pivotal for boosting accuracy in small medical image datasets. The use of feature fusion and systematic evaluation across color spaces highlights the importance of input representation and network architecture, offering valuable insights for future improvements. While the results are promising, direct comparison with published SOTA methods underscores some areas for potential enhancement: Future work should integrate advanced data augmentation, ensemble models, and transformer-based architectures that have demonstrated superior performance in recent literature. Further benchmarking against the latest reported results on the BACH dataset, including both accuracy and computational efficiency metrics, will provide additional validation and highlight the practical value of the proposed approach. The current method surpasses traditional single-CNN pipelines and provides a robust baseline for breast cancer classification on the BACH dataset. However, there remains a clear opportunity for further improvement through the adoption of advanced techniques seen in recent SOTA models. Explicit comparative benchmarking and the application of these latest strategies are recommended for future research directions.

## Acknowledgment

To ensure scientific accuracy, verify the correctness of references, and review translations, we employed AI tools, including ChatGPT and Perplexity, thereby minimizing the potential for scientific errors.

## References

[1] S. Lee and C. A. Schmitt, "The dynamic nature of senescence in cancer," *Nature cell biology,* vol. 21, no. 1, pp. 94-101, 2019.

[2] B. Weigelt, J. L. Peterse, and L. J. Van't Veer, "Breast cancer metastasis: markers and models," *Nature reviews cancer,* vol. 5, no. 8, pp. 591-602, 2005.

[3] A. N. Giaquinto *et al.*, "Breast cancer statistics 2024," *CA: a cancer journal for clinicians,* vol. 74, no. 6, pp. 477-495, 2024.

[4] F. Roshanravan Yazdi, M. M. Khalilzadeh, F. Firouzi, and M. Azarnoosh, "Breast mass detection with nonlinear model of thermography images," *Contributions of Science and Technology for Engineering,* 2025.

[5] F. R. Yazdi, M. M. Khalilzadeh, F. Firouzi, and M. Azarnoosh, "Evaluation of Breast Thermography Images according to Ultrasound Reports and Temperature Pattern: Evaluating breast thermography images," *Archives of Breast Cancer,* vol. 12, no. 2, pp. 187-194, 2025.

[6] Z. Rezaei, "A review on image-based approaches for breast cancer detection, segmentation, and classification," *Expert Systems with Applications,* vol. 182, p. 115204, 2021.

[7] Z. He *et al.*, "A review on methods for diagnosis of breast cancer cells and tissues," *Cell proliferation,* vol. 53, no. 7, p. e12822, 2020.

[8] S. Alimirzaie, M. Bagherzadeh, and M. R. Akbari, "Liquid biopsy in breast cancer: A comprehensive review," *Clinical genetics,* vol. 95, no. 6, pp. 643-660, 2019.

[9] A. Soliman, Z. Li, and A. V. Parwani, "Artificial intelligence's impact on breast cancer pathology: a literature review," *Diagnostic pathology,* vol. 19, no. 1, p. 38, 2024.

[10] X. Y. Liew, N. Hameed, and J. Clos, "A review of computer-aided expert systems for breast cancer diagnosis," *Cancers,* vol. 13, no. 11, p. 2764, 2021.

[11] N. Safdarian and M. Hedyezadeh, "Detection and classification of breast cancer in mammography images using pattern recognition methods," *Multidisciplinary Cancer Investigation,* vol. 3, no. 4, pp. 13-24, 2019.

[12] F. F. Ting, Y. J. Tan, and K. S. Sim, "Convolutional neural network improvement for breast cancer classification," *Expert Systems with Applications,* vol. 120, pp. 103-115, 2019.

[13] A. H. Song *et al.*, "Artificial intelligence for digital and computational pathology," *Nature Reviews Bioengineering,* vol. 1, no. 12, pp. 930-949, 2023.

[14] Y. Zhou, C. Zhang, and S. Gao, "Breast cancer classification from histopathological images using resolution adaptive network," *IEEE Access,* vol. 10, pp. 35977-35991, 2022.

[15] G. Aresta *et al.*, "Bach: Grand challenge on breast cancer histology images," *Medical image analysis,* vol. 56, pp. 122-139, 2019.

[16] X. Xiong *et al.*, "Breast cancer: pathogenesis and treatments," *Signal transduction and targeted therapy,* vol. 10, no. 1, p. 49, 2025.

[17] T. J. Key, P. K. Verkasalo, and E. Banks, "Epidemiology of breast cancer," *The lancet oncology,* vol. 2, no. 3, pp. 133-140, 2001.

[18] M. Kowal, P. Filipczuk, A. Obuchowicz, J. Korbicz, and R. Monczak, "Computer-aided diagnosis of breast cancer based on fine needle biopsy microscopic images," *Computers in biology and medicine,* vol. 43, no. 10, pp. 1563-1572, 2013.

[19] S. B. Shamir, A. L. Sasson, L. R. Margolies, and D. S. Mendelson, "New frontiers in breast cancer imaging: the rise of AI," *Bioengineering,* vol. 11, no. 5, p. 451, 2024.

[20] N. K. Tyagi and S. Dhesy-Thind, "Clinical practice guidelines in breast cancer," *Current Oncology,* vol. 25, no. Suppl 1, p. S151, 2018.

[21] S. L. Goff and D. N. Danforth, "The role of immune cells in breast tissue and immunotherapy for the treatment of breast cancer," *Clinical breast cancer,* vol. 21, no. 1, pp. e63-e73, 2021.

[22] M. Gupta and N. Goyal, "Applied anatomy of breast cancer," in *Breast Cancer: Comprehensive Management*: Springer, 2022, pp. 23-35.

[23] S. A. Zendehbad and J. Ghasemi, "Advanced Deep Learning Approaches for Accurate and Efficient Suspicious Behavior Detection in Surveillance Videos," *Computational Sciences and Engineering,* 2025.

[24] H. Hosseinpour, J. Ghasemi, and F. Abesi, "Analysis of Panoramic Dental Images for Dental Symptom Differentiation Based on Deep Learning," *Future Research on AI and IoT,* vol. 1, no. 1, pp. 1-9, 2025.